19th Annual Meeting of the Institute of Liquid Atomization and Spray Systems (Europe)
Nottingham, 6-8 September 2004

SPRAY IMPINGEMENT HEAT TRANSFER MODEL

J. C. Landero and A. Paul Watkins

Department of Mechanical, Aerospace & Manufacturing Engineering, UMIST
Manchester M60 1QD, UK.

Paul.Watkins@umist.ac.uk.

ABSTRACT

A new Spray Impingement Heat Transfer Model (SIHTM), has been developed on the basis of the engineering superposition principle. The model predicts the steady state heat flux from a hot surface to the spray for the three heat transfer boiling regimes under the following droplet impinging Weber number and wall temperature ranges: $0< We <1000$ and $373< T_{wall} <573$, under normal pressure conditions. In the SIHTM the heat transfer and drop hydrodynamic phenomena occurring during spray cooling are intimately related but not coupled. In order to have these phenomena independent, impaction-behaviour data was extracted from third parties' experimental works, and transient heat transfer data was obtained by means of an in-house computational code called Layer. The model performance was tested against spray cooling experimental data. One major set of steady state experimental heat transfer data has been used to assess the accuracy of the computer model. The data was obtained from four full cone water atomizers [1], which were used to experimentally cool a heated test piece. The spray cooling experiment also used different impaction distances, injection pressures, and wall temperatures. Steady state heat transfer rates were measured [2]. The heat transfer model predictions were compared to eighteen different spray cooling experimental conditions and reasonable agreement was obtained.

INTRODUCTION

Spray cooling of heated surfaces using water is commonly used in some industrial applications, one of which is steel making. Within this industrial activity spray cooling has proved to be convenient because of its low operating costs, high heat dissipation capabilities, and its versatility to be adapted to different geometrical configurations. In continuous steel casting processes the settings of the spray cooling system are varied to match the type of steel to be cast and the casting speed of the line. These multi-settings spray cooling systems have to be technically specified in advance, and in order to do so the prediction of the steady state heat transfer process between the hot metal surface and the water spray at different thermal conditions is crucial. The SIHTM is capable of predicting the steady state heat flux from the hot surface to the spray in such conditions.

Two facts greatly influenced the model's development process: 1) the necessity of predicting steady state heat fluxes between sprays having different spray characteristics, and walls at different surface temperatures, and 2) the need for low computational costs (computational calculation time, and memory requirements). In order to satisfy these two requirements the model accounts for the three boiling regimes (nucleate, transition, and film boiling), and works in the following droplet impinging Weber numbers and wall temperature ranges: $0< We <1000$ and $373< T_{wall} <573$, under normal pressure conditions. The transient heat transfer process between the drops and the wall, and drop impaction-behaviour phenomena were decoupled but designed to be intimately related instead, thereby reducing the computational costs. The impaction-behaviour data were extracted from third parties' experimental works, and transient heat transfer data were obtained by means of an in-house computational code called Layer.

SPRAY IMPINGEMENT HEAT TRANSFER MODEL

Impaction-Behaviour Data

The impaction-behaviour life of any drop impinging on a hot wall was divided into three time periods (see Table 1) using the non-dimensional spread ratio number, $\beta = D/d_0$, which is the ratio of the splat diameter to the drop original diameter, as the defining parameter of the time periods. Once the time periods were defined, the actual times were extracted from experimental data obtained by Bernardin et al [3], and Chandra et al [4] on the impaction process on hot surfaces.

Information about the spreading process of drops impinging on walls at different surface temperatures was provided by Chandra et al [4] for drops with $We = 43$. Assuming that a spread ratio curve $\beta = f(t)$ reaches higher values as the drop impinging Weber number increases a sizing factor was used to extrapolated the data provided by Chandra et al [4] to drops impinging the wall at Weber numbers different to 43, allowing the following relations to be predictable,

(1)

$$t_{\beta=1} = f(We, T_{wall})$$

(2)

$$\beta = f(We, T_{wall}, t)$$

Information about the end of the spreading process ($t_{\beta=\beta\max}$), and the end of contact between the drop and the wall (by evaporation, or rebound, or break-up), for different wall temperature conditions was extracted from the experimental work of Bernardin et al [3]. This information was provided only for drops impinging the wall with *We* = 20, 60, 220, and was therefore interpolated and extrapolated here to predict impinging conditions for other Weber numbers. Then from this experimental work the following relations became predictable.

(3)

$$t_{\beta=\beta\max} = f(We, T_{wall})$$

(4)

$$t_{end} = f(We, T_{wall})$$

With the information predicted by equations (1-4) for each drop impinging the wall in the wall temperature range and Weber number range of the SIHTM, the three time periods of the impaction-behaviour could be defined and average heat fluxes could be calculated for each of them.

Table 1. Definition of the Time Periods into which the Impaction-Behaviour Lifetime of a Drop was Divided.

First Time Period	$t_{\beta=0} - t_{\beta=1}$
Second Time Period	$t_{\beta=1} - t_{\beta=\beta\max}$ (During this period the spreading process takes place)
Third Time Period	$t_{\beta=\beta\max} - t_{end}$ (The end could result from drop evaporation, break-up, or rebound)

Heat Transfer Data

Transient heat transfer data was numerically obtained by the use of an in-house computational code named LAYER. Static liquid films of different heights (1μm < radius < 249μm), the same range as for the drop diameter, heated over a constant temperature wall were tested for 11900 different wall temperature, liquid film temperature, and liquid film height initial conditions, obtaining a heat transfer database having average heat fluxes (W/m^2), and specific points in time within the heating process of the liquid films. The liquid films were subjected to convection with the hot wall, and the surrounding air. Bi-dimensional conduction equations were used to model the temperature profile development within the liquid (conduction equations have already been used by [5], and [6] for similar modelling purposes). All liquid films were vertically divided into 65 layers of the same length to model with more precision the temperature profile within them (See Figure 1). Special attention was paid to the layer in contact with the surface (first layer), which governed the end of calculation. Two specific points in time within the liquid film temperature profile development process were recorded: 1) the time at which the first layer reached the saturation temperature (t_{sat}), and 2) the time at which the first layer evaporated (t_{evap}). For each of these two specific points in time average heat fluxes were also obtained. A fifth output quantity was recorded from the computational simulation: the temperature profile of the film at the first layer evaporation time.

The wall temperature conditions tested by the program varied from 373 K to 573 K in increments of 10 K. The initial liquid film temperature conditions tested varied from 292.15 K to 372.15 K, in increments of 5 K. The liquid film radii tested were from 1 – 49 μm in steps of 2 μm, and from 49 – 249 μm, in steps of 20 μm. Taking into account all the combinations of initial liquid film temperature, wall temperature, and liquid film radius 20x17x35=11900 calculations were performed.

The heat transfer data obtained by computational simulation in program LAYER assumed for the entire range of wall temperatures that the liquid film was in touch with the hot wall (in the real case a vapour cushion appears between the liquid and the wall in the transition and film boiling regimes), so as the wall temperature increased the heat fluxes increased too. In order to model the real behaviour, the appearance of the vapour cushion beneath the liquid film in the transition and film boiling regimes had to be taken into account. It was assumed that the decay in the heat flux values between the wall and the liquid film in these regimes was solely due to the appearance of this vapour cushion, whose frequency of appearance increased as the wall temperature increased (i.e. the vapour cushion presence had lower frequencies of appearance in the transition boiling regime, and higher in the film boiling regime). To model this phenomenon a vapour cushion presence factor, based on thermal boundary layer theory, was developed and applied to the heat transfer data for high surface temperatures conditions.

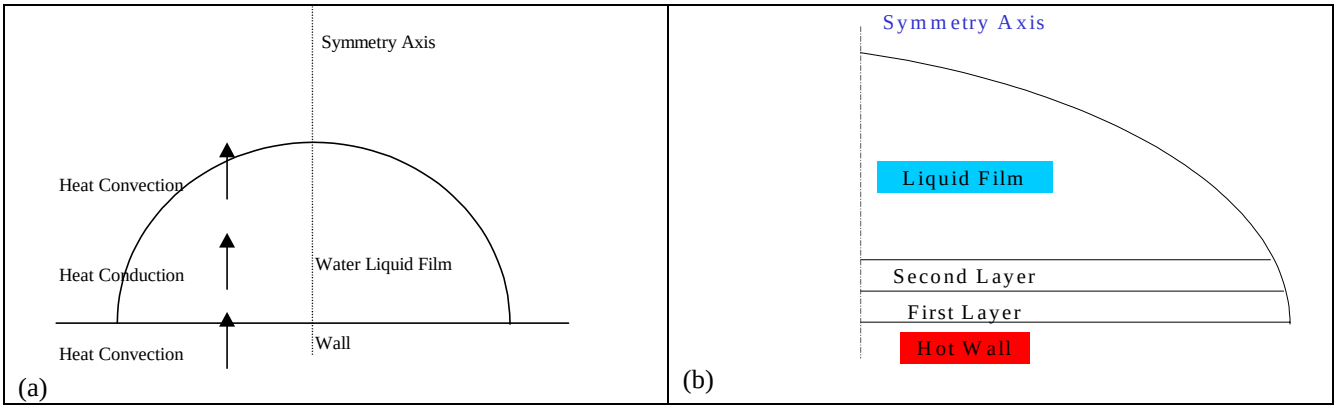

Figure 1. (a) Schematic diagram of a liquid film showing the heat fluxes modelled, (b) Schematic diagram of half a liquid film showing the disposition and placement of the layers.

Spray Impingement Heat Transfer Model

In the previous sections the impaction-behaviour data and transient heat transfer data were described, as well as the experimental and computational works they were obtained from. This section will explain briefly how they are related in order to predict the spray impingement heat transfer phenomenon. The spray heat flux is calculated as the average heat flux of the spray over a certain number of the spray code's time steps.

(5)

$$q''_{spray} = \frac{\sum_{m=1}^{a} q''_{m\_spray\_per\_time\_step}}{a}$$

Where a is the integer number of time steps calculated. In a similar way the spray heat flux per time step is the average wall-cell heat flux,

(6)

$$q''_{spray\_per\_time\_step} = \frac{\sum_{n=1}^{b} q''_{n\_wall-cell}}{b}$$

where b is the number of wall-cells calculated. Within each wall-cell the heat flux can be calculated either in flooded condition or in non-flooded condition. The flooded condition merges all the droplets in a particular wall-cell so a liquid film is formed over it, then the heat flux is calculated from the hot surface to this liquid film.

(7)

$$q''_{wall-cell} = q''_{liquid\_film}$$

The non-flooded condition treats each droplet within the wall-cell as an independent liquid mass, so the heat flux is calculated on a droplet-by-droplet basis, and the average heat flux to all droplets within a wall-cell gives then the wall-cell's heat flux.

(8)

$$q''_{wall-cell} = \frac{\sum_{o=1}^{c} q''_{o\_droplets}}{c}$$

where c is the number of droplets present in a particular non-flooded wall-cell. The heat flux from the hot wall to a liquid film q''_{liquid_film}, or to a droplet $q''_{droplet}$, having the same initial liquid and wall temperature conditions are calculated using the same procedure, intimately relating the impaction-behaviour data and the transient heat transfer data. This is due to the fact that heat fluxes are being calculated (W/m^2), so the larger area occupied by a liquid film makes no difference.

The procedure to calculate heat fluxes relating the impaction-behaviour data and the heat transfer data is as follows:

In the interaction time of a droplet or liquid film with the hot surface, three time periods were defined. A heat flux for each of them is calculated (i.e. q''_1 for the first time period heat flux, q''_2 for the second time period …)

(9)

$$q''_{liquid\_film\_or\_droplet} = \frac{q''_1 + q''_2 + q''_3}{3}$$

Within each time period several of the 65 layers of a drop or liquid film could have been evaporated, so a time period heat flux is in itself an average of the heat flux transferred from the hot surface to all layers of the droplet or liquid film that have been in contact with the hot surface within it. See next equation as an example:

(10)

$$q''_1 = \frac{\sum_{p=1}^{d} q''_{p\_layers}}{d}$$

where d is the number of layers of a drop or liquid film that have been in contact with the hot surface. The data to calculate the heat flux from the hot surface to the layers of the droplet or liquid film in contact with it are taken from the heat transfer database where 11900 different thermal conditions calculated by program LAYER are stored.

When a drop or liquid film starts its heating process its height, liquid temperature, and wall temperature are taken into account to retrieve the appropriate information from the heat transfer database. Once a layer of the drop or liquid film is evaporated, the temperature profile of it is consulted to know which is the final temperature of the subsequent layer (the layer on top of the one evaporated) because it will provide the liquid temperature for the new thermal condition. Changes in the wall temperature can also be checked, if they exist.

RESULTS AND DISCUSSION

Yule et al [1], and Nasr et al [7], measured the spray characteristics of four commercial full cone atomisers for water supply pressures of 0.69, 1.38, and 2.07MPa, for exit orifice diameters of 0.61, 0.94, 1.19, and 1.70mm, and for an initial spray angle of $56^0 \pm 8^0$. The range of impaction distances tested for these atomisers were 140, 240, 340, and 440 mm.

Jeong [8], and Sharief et al [2], obtained comprehensive quantitative information regarding the parameters affecting spray cooling using the four full cone atomizers described above. Heat transfer characteristics in the range of surface temperature 100^0C to 1000^0C were investigated under steady state conditions. The range of parameters considered were 0.23 to 3.32 kg/m^{2}s for mass flux, 34.7 to 128 μm for drop median diameter and 7.05 to 23.10 m/s for impinging velocity, giving eighteen experimental cases to compare with the numerical predictions of the SIHTM.

Figures 2 to 4 show the comparison between the experimental steady state heat flux, and the numerically predicted steady state heat flux for three out of eighteen cases. Each numerical prediction point in the graphs is an independent CFD calculation. The calculations started once the spray had impinged the wall and steady state conditions had been reached (velocity and pressure values for the gas phase were monitored in different places of the chamber). The CPU cost of each point varied from 15 to 45 minutes depending on the injector to wall distance, and the injector pressure (larger impingement distances, and lower pressure values resulted in larger CPU costs).

Generally speaking the trend of the numerical predictions show as expected well defined critical heat flux points, Leidenfrost points, as well as an appropriate decay of the heat flux between them (i.e. the transition boiling regime is reasonably well predicted). In the majority of the cases the critical heat flux point was predicted around the 473 K wall temperature (100 K of wall superheat). The Leidenfrost point predictions appeared around the wall temperature value of 553 K for most cases (180 K of wall superheat, almost 100 K after the appearance of the critical heat flux point predictions).

In general terms the experimental data cases show a flatter trend than that of the numerical predictions. This trend discrepancy between the experimental data and the numerical predictions could be the result of basing the numerical predictions on a boiling curve for stagnant liquid conditions. Nevertheless the fact that the numerical predictions show a similar trend to that of the experimental boiling curve supplies evidence that the use of the vapour-cushion presence factor gives good results. When comparing the magnitudes of the heat flux between the experimental data and the numerical predictions it was found that nine out of eighteen cases over predicted it, seven out of eighteen were found similar in magnitude (as the three cases shown here), and two out of eighteen under predicted it [9].

The majority of the cases in which the numerical method over predicted the heat flux are found to be those in which the test piece was set at the larger distances from the nozzle, and they also had a low injection pressure. These two circumstances produce drops that are relatively large due the low injection velocity, and with the effects of drop break-up minimized. The impaction velocities will also be relatively small. However, it is not clear why these effects should result in the observed trend.

Another possible explanation is that the predictions are based on the assumption of uniform mass flux across the nozzle. In reality wide-angle sprays have a relatively dilute core region that may extend back to the nozzle. Thus in the

predictions the core region impacting on the test piece may contain too much mass, hence increasing the heat flux predictions over the experimental values. This would particularly be the case when the test piece is at a large distance from the nozzle.

Almost all of the test cases in which the agreements between the predictions and experiments are best, are found to be those in which the injection pressure has the highest value employed (Fig. 4 is an exception). Thus it can be concluded that the injection pressure plays a major role in whatever deficiency exists in the model. This again may be connected to the mass flow rate, which is strongly effected by this parameter. The higher injection pressures will also result in a finer, more mono-dispersed spray. Both short distance and long distance test cases are included in this category, in virtually equal measure, so clearly this parameter is not influential when employing high injection pressures.

No correlation could be found between the level of agreement between the predictions and experiment and the nozzle diameter.

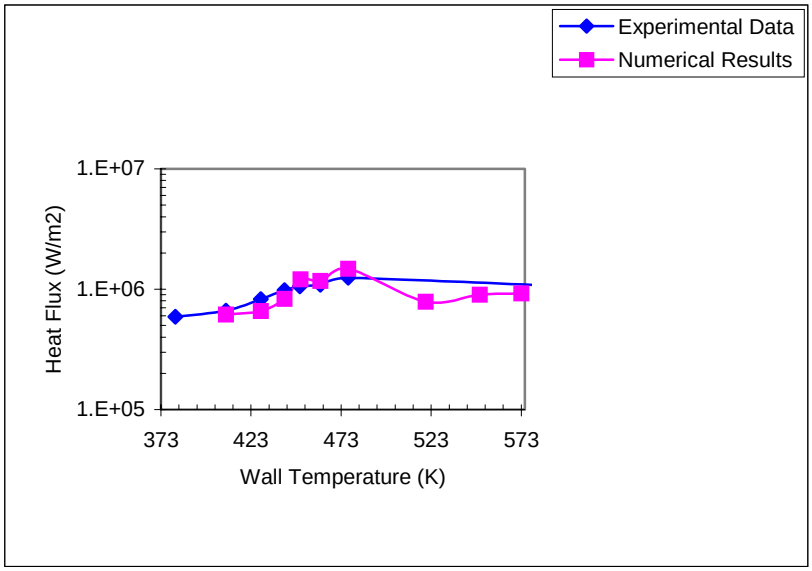

Figure 2. Comparison of the experimental steady state heat flux against the numerical prediction. Nozzle diameter 0.61 mm, injection pressure 2.07 MPa, impaction distance 140 mm.

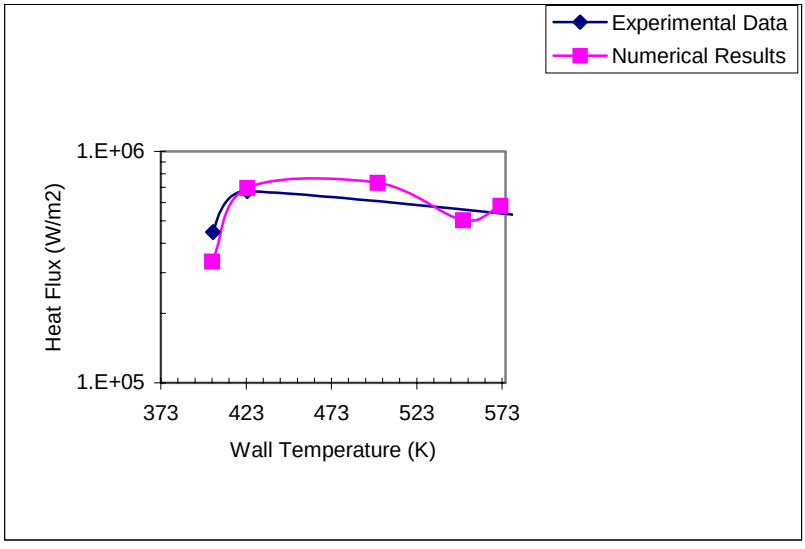

Figure 3. Comparison of the experimental steady state heat flux against the numerical prediction. Nozzle diameter 0.61 mm, injection pressure 2.07 MPa, impaction distance 240 mm.

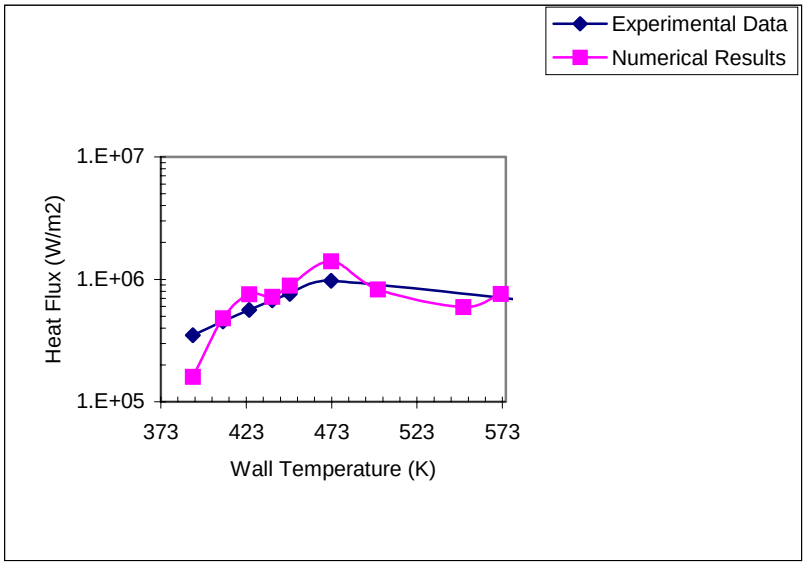

Figure 4. Comparison of the experimental steady state heat flux against the numerical prediction. Nozzle diameter 0.94 mm, injection pressure 0.69 MPa, impaction distance 240 mm

CONCLUSIONS

The SIHTM was presented. The model is based on the engineering superposition principle linking impaction-behaviour data of drops over hot surfaces, and transient heat transfer data. The result of joining of these two sets of data allows the prediction of steady state heat fluxes between sprays of different characteristics and hot walls with different surface temperatures. The model has been compared to eighteen experimental cases, three of which have been presented here. Reasonable accuracy between the predictions and the experimental work was found. The level of agreement between the predictions and experiment was found to depend most strongly on the injection pressure, with higher injection pressures generally leading to better agreement. This might be due to having a finer, more mono-dispersed spray. The mass flux impacting on the surface is clearly of paramount importance, and it may be that an incorrect assumption of uniform mass flux across the nozzle plays a role in determining the accuracy of the model.

REFERENCES

1. Yule, A.J., Jeong, J.R., James, D.D., Nasr, G.G., Sharief, R.A., The performance characteristics of solid cone spray pressure swirl atomisers. Atomization and Sprays, Vol. 10, pp. 627-646, 2000.
2. Sharief, R.A., Nasr, G.G., Yule, A.J., Widger, I.R., Jeong, J.R., James, D.D., Steady state high pressure spray cooling of high temperature steel surfaces. ICLASS-2000, Pasadena, Ca., USA, 2000.
3. Bernardin, J.D., Stebbinds, C.J., Mudawar, I., Mapping of impact and heat transfer regimes of water drops impinging on a polished surface. Int. J. Heat Mass Transfer, Vol. 40, No. 2, pp. 247-267, 1997.
4. Chandra, S., and Avedisian, C.T., On the collision of a droplet with a solid surfaces. Proc. R. Soc. London A, Vol. 432, pp. 13-41, 1991.
5. Pasandideh-Fard, M., Aziz, S.D., Chandra, S., Mostaghimi, J., Cooling effectiveness of a water drop impinging on a hot surface. International Journal of heat and Fluid Flow, Vol. 22, pp. 201-210, 2001.
6. Di Marzo, M., Tartarini, P., Liao, Y., Evans, D., Baum, H., Evaporative cooling due to a gently deposited droplet. Int. J. Heat Transfer, Vol. 36, No. 17, pp. 4133-4139, 1993.
7. Nasr, G.G., Sharief, R.A., James, D.D., Jeong, J.R., Widger, I.R., Yule, A.J., Studies of high pressure water sprays from full-cone atomizers. 15th Annual Conference Liquid Atomization Spray Systems-Europe, Toulouse, France, 1999.
8. Jeong, J.R., High pressure spray cooling of high temperature steel surfaces. M.Phil. Thesis, UMIST, Manchester, UK, 1999.
9. Landero, J.-C., Spray-impingement heat transfer model. Ph.D. Thesis, UMIST, Manchester, UK, 2004.